Johannes Böhm, Birgit Werl, and Harald Schuh

Troposphere mapping functions for GPS and VLBI

from ECMWF operational analysis data

2006a

Troposphere mapping functions for GPS and VLBI from ECMWF operational analysis data

Johannes Böhm, Birgit Werl, and Harald Schuh

Abstract

In the analyses of geodetic VLBI and GPS data the analytic form used for mapping of the atmosphere delay from zenith to the line-of-site is most often a three parameter continued fraction in 1/sin(elevation). Using the 40 years reanalysis (ERA-40) data of the ECMWF (European Centre for Medium-Range Weather Forecasts) for the year 2001, the b and c coefficients of the continued fraction form for the hydrostatic mapping functions have been re-determined. Unlike previous mapping functions based on data from numerical weather models (Isobaric Mapping Functions IMF [*Niell*, 2000], Vienna Mapping Functions VMF [*Boehm and Schuh*, 2004]), the new c coefficients are dependent on the day of the year, and unlike the Niell Mapping Functions NMF [*Niell*, 1996] they are no longer symmetric with respect to the equator (apart from the opposite phase for the two hemispheres). Compared to VMF, this causes an effect on the VLBI or GPS station heights which is constant and as large as 2 mm at the equator and which varies seasonally between 4 mm and 0 mm at the poles. The updated VMF, based on these new coefficients and called VMF1 hereafter, yields slightly better baseline length repeatabilities for VLBI data. The hydrostatic and wet mapping functions are applied in various combinations with different kinds of a priori zenith delays in the analyses of all VLBI IVS-R1 and IVS-R4 24-hour sessions of 2002 and 2003; the investigations concentrate on baseline length repeatabilities, as well as on absolute changes of station heights.

1 Introduction

Modeling the path delays due to the neutral atmosphere for microwave signals emitted by satellites or radio sources is one of the major error sources in the analyses of Global Positioning System (GPS) and Very Long Baseline Interferometry (VLBI) observations. The concept is based on the separation of the path delays, ∆L, into a hydrostatic and a wet part [e.g., *Davis et al.*, 1985].

(1) $\Delta L(e) = \Delta L_h^z \cdot mf_h(e) + \Delta L_w^z \cdot mf_w(e)$

In equation 1, the total delays $\Delta L(e)$ at an elevation angle e are made up of a hydrostatic (index h) and a wet (index w) part, and each of these terms is the product of the zenith delay (ΔL_h^z or ΔL_w^z) and the corresponding mapping function mf_h or mf_w. These mapping functions, which are independent of the azimuth of the observation, have been determined for the hydrostatic and the wet part separately by fitting the coefficients a, b, and c of a continued fraction form [*Marini*, 1972] (equation 2) to standard atmospheres [e.g., *Chao*, 1974], to radiosonde data [*Niell*, 1996], or recently to numerical weather models (NWMs) [e.g., *Niell*, 2000; *Boehm and Schuh*, 2004].

(2) $mf(e) = \dfrac{1 + \dfrac{a}{1 + \dfrac{b}{1+c}}}{\sin e + \dfrac{a}{\sin e + \dfrac{b}{\sin e + c}}}$

Whereas the hydrostatic zenith delays, ΔL_h^z (m), which can be determined from the total pressure p in hPa and the station coordinates (latitude φ and height h in m) at a site [*Saastamoinen*, 1973] (equation 3), and the hydrostatic and wet mapping functions are assumed to be known, the wet zenith delays, ΔL_w^z, are estimated within the least-squares adjustment of the GPS or VLBI analyses.

(3) $\Delta L_h^z = 0.0022768 \cdot \dfrac{p}{\left(1 - 0.00266 \cdot \cos(2\varphi) - 0.28 \cdot 10^{-6} \cdot h\right)}$

However, there might be errors in the hydrostatic zenith delays or the mapping functions, and their influence on station heights is well described with a rule of thumb by *Niell et al.* [2001]: *The error in the station height is approximately one third of the delay error at the lowest elevation angle included in the analysis.* Following a refinement of this rule of thumb by *Boehm* [2004], the factor is rather 1/5 than 1/3 for a minimum elevation angle of 5°, which is also close to the value 0.22 found by *MacMillan and Ma* [1994]. The following two examples illustrate this rule of thumb, which holds for both GPS and VLBI, but which depends on the actual distribution of elevations and on whether elevation-dependent weighting is used: The

hydrostatic and wet zenith delays are taken to be 2000 mm and 200 mm, respectively, the minimum elevation angle is 5°, and the corresponding values for the hydrostatic and wet mapping functions are 10.15 ($mf_h(5°)$) and 10.75 ($mf_w(5°)$). (1) We assume an error in the total pressure measured at the station of 10 hPa: 10 hPa correspond to ~20 mm hydrostatic zenith delay (compare equation 3), which is then mapped down with the wrong mapping function (factor 0.6 = 10.75 −10.15). At 5° elevation the mapping function error is 12 mm, and one fifth of it, i.e. 2.4 mm, would be the resulting station height error. (2) We consider an error in the wet mapping function of 0.01 ($mf_w(5°)$ = 10.76 instead of 10.75) or in the hydrostatic mapping function of 0.001 ($mf_h(5°)$ = 10.151 instead of 10.15). The error at 5° elevation in both cases is 20 mm, i.e. the error in the station height would be approximately 4 mm.

The Vienna Mapping Functions (VMF) introduced by *Boehm and Schuh* [2004] depend only on elevation angle and not on azimuth, i.e. they assume that the troposphere is symmetric around the stations. For the b and c coefficients (see equation 2) the best values available at that time were taken from the Isobaric Mapping Functions (IMF) [*Niell and Petrov*, 2003] for the hydrostatic part and from the Niell Mapping Functions (NMF) at 45° latitude [*Niell*, 1996] for the wet part. Figure 8 shows the hydrostatic mapping function from NMF and VMF for the station Algonquin Park in 2002 and 2003. In section 2, an updated version for the VMF [*Boehm and Schuh*, 2004] is developed, which is based on new b and c coefficients for the hydrostatic mapping functions and which will be called VMF1 hereafter. For VMF1, the c coefficients from raytracing are fit to a function of latitude and day of year to remove systematic errors. This is important for geophysical applications of geodesy, for instance, to determine the correct seasonal and latitude dependence of hydrology. An alternative approach to the traditional separation into wet and hydrostatic mapping functions is the introduction of the 'Total' Vienna Mapping Function' (VMF1-T) for mapping down the total delays, which uses the total refractivity instead of its hydrostatic and wet components. In section 3 different procedures are described for calculating a priori zenith delays that can be used for GPS and VLBI analyses, including their determination from the operational analysis pressure level dataset of the ECMWF (European Centre for Medium-Range Weather Forecasts). In section 4, the impact of the different mapping functions and of the different a priori zenith delays on geodetic results is investigated using all IVS-R1 and IVS-R4 24-hour sessions of 2002 and 2003, including CONT02. CONT02 was a two-week continuous VLBI campaign in the second half of October 2002 [*Thomas and MacMillan*, 2003].

2 New hydrostatic b and c coefficients for VMF1

At the ECMWF, the ERA-40 (ECMWF Re-Analysis 40-years) data are stored as expansions of spherical harmonics with a horizontal resolution corresponding to about 125 km [*Simmons and Gibson*, 2000]. From these data, monthly mean profiles for the year 2001 (for the epochs 0, 6, 12, and 18 UT) were downloaded on a global grid (30° in longitude by 15° in latitude). These profiles consist of 23 levels from 1000 hPa to 1 hPa (1000, 925, 850, 775, 700, 600, 500, 400, 300, 250, 200, 150, 100, 70, 50, 30, 20, 10, 7, 5, 3, 2, 1), and they comprise values for height, total pressure, temperature, and water vapor pressure for each level.

2.1 Determination of the b and c coefficients

In a first step, for all 7488 profiles (156 grid points times 12 months times 4 epochs per day) the total and hydrostatic mapping functions as well as the vacuum elevation angles e are determined for 10 different initial elevation angles e_0 (3.2°, 5°, 7°, 10°, 15°, 20°, 30°, 50°, 70°, 90°) [compare *Boehm*, 2004]. The vacuum elevation is the asymptotic final elevation angle of the outgoing ray and corresponds to the direction expected for the target observed, either the GPS satellite or the VLBI radio source. The geometric bending effect ΔL_{bend} [see *Davies et al.*, 1985] is added to the hydrostatic and to the total mapping functions (equations 4 and 5).

$$(4) \qquad mf_h(e) = \frac{\Delta L_h(e) + \Delta L_{bend}(e)}{\Delta L_h^z}$$

$$(5) \qquad mf_t(e) = \frac{\Delta L_h(e) + \Delta L_w(e) + \Delta L_{bend}(e)}{\Delta L_h^z + \Delta L_w^z}$$

Then, the three coefficients a, b, and c of the total and hydrostatic mapping functions (equation 2) are fitted to the ten discrete mapping function values of each profile by a least-squares adjustment. The residuals of their fit are usually smaller than 0.5 mm. These 7488 mapping functions will be used as 'rigorous' reference for evaluations in section 2.2. The mean value of all b coefficients for both the total (index t) and hydrostatic (index h) mapping functions is found to be

(6) $b_t = b_h = 0.0029$,

and is kept fixed in all further analyses. In the next step the least-squares adjustment is repeated, but only the coefficients a and c are estimated for all profiles, while the coefficient b for the hydrostatic and total mapping functions is kept fixed to the value given in equation 6. The coefficients c then show a clear variability depending on season and latitude, but unlike former mapping functions, the coefficients c are not symmetric with respect to the equator (apart from the phase offset for the two hemispheres). For example, the coefficient c at the North pole in January is significantly smaller than c at the South pole in July (figure 1). Therefore, equation 7 is used to model the coefficient c, when doy is the day of the year and 28 January has been adopted as the reference epoch [*Niell*, 1996], φ is the latitude, and ψ specifies the northern or southern hemisphere (see the last columns of table 1 and 2).

(7) $c = c_0 + \left[\left(\cos\left(\dfrac{doy - 28}{365} \cdot 2\pi + \psi \right) + 1 \right) \cdot \dfrac{c_{11}}{2} + c_{10} \right] \cdot (1 - \cos\varphi)$
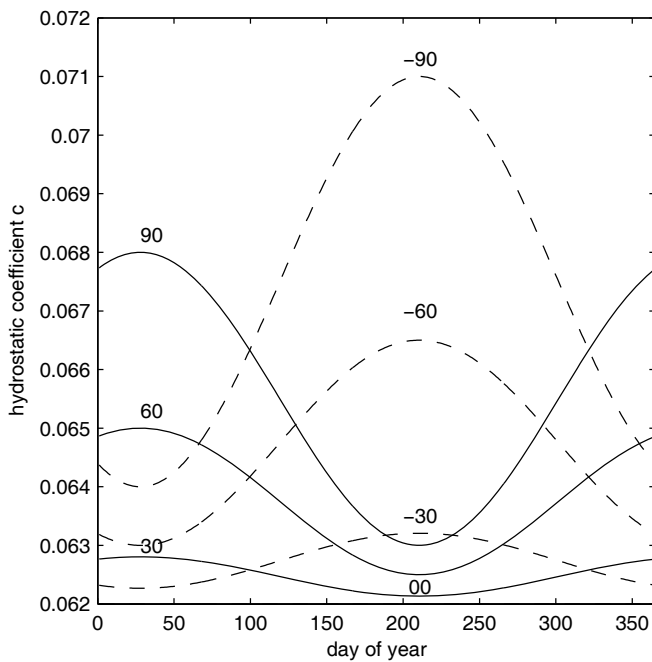

Figure 1. Hydrostatic coefficients c for 0°, ±30°, ±60°, and ±90° latitude in 2001 from ERA-40 data (equation 7).

Table 1 and table 2 contain the parameters of equation 7 which are obtained for the hydrostatic and total mapping functions. As an example, the coefficient c in January 2001 is plotted in figure 1 for different latitudes.

Table 1. Parameters c_0, c_{10}, c_{11}, and ψ needed for computing the coefficient c (eq. 7) of the hydrostatic mapping function (eq. 4).

hemisphere	c_0	c_{10}	c_{11}	ψ
northern	0.062	0.001	0.005	0
southern	0.062	0.002	0.007	π

Table 2. Parameters c_0, c_{10}, c_{11}, and ψ needed for computing the coefficient c (eq. 7) of the total mapping function (eq. 5).

hemisphere	c_0	c_{10}	c_{11}	ψ
northern	0.063	0.000	0.004	0
southern	0.063	0.001	0.006	π

The b and c coefficients of the wet mapping functions do not have to be changed because the wet zenith delays are smaller by a factor of ~10 than the hydrostatic zenith delays and the effect of variations in b and c is not significant. The b and c coefficients of the wet mapping function are still fixed to those of NMF [*Niell*, 1996] at 45° latitude and the coefficient a is estimated for each profile, i.e., the recommended wet mapping function is still VMF(wet).

2.2 Evaluation of the new coefficients

The 'fast' approach (in which the parameter a is estimated from a single raytrace at initial elevation angle $e_0 = 3.3°$) can be compared with the 'rigorous' approach that determines all three coefficients in a least-squares adjustment using ten different initial elevation angles. The maximum differences are encountered at 5° elevation because the 'fast' mapping functions (VMF1) are 'tuned' for elevations of ~3°, i.e. there is no error at ~3°, while at elevation angles considerably higher than 5° the differences between the rigorous and the fast approach are also vanishing. With the new b and c coefficients (equation 7 and tables 1 and 2), the deviation from the rigorous approach at 5° elevation is always smaller than 8 mm, which means that the corresponding error in the station height is always smaller than 1.6 mm. This holds for all months in 2001 and for all latitudes and longitudes (see table 3).

Table 3. Mean biases and standard deviations of hydrostatic delay differences at 5° elevation for NMF, VMF, and VMF1 with respect to the hydrostatic mapping functions derived from the numerical weather model for a global grid and 12 months in 2001. In parentheses the equivalent station height errors are given.

	mean bias [mm]	standard deviation [mm]
NMF	21.8 (4.4)	35.0 (7.0)
VMF	3.3 (0.7)	11.2 (2.2)
VMF1	2.3 (0.5)	2.0 (0.4)

The principle of VMF1 (which is the principle of VMF(fast) in [*Boehm and Schuh*, 2004]) is to use the best coefficients b and c available, determine the values of the mapping functions at $e_0 = 3.3°$ initial elevation angle from the NWM, and derive the coefficient a by simply inverting the continued fraction form (equation 2). In our study, the values of the mapping functions for the VLBI and GPS stations are determined from the ECMWF operational pressure level data. No horizontal interpolation for the sites has to be done between grid points because the latitudes and longitudes of the stations are input parameters to the expansion of spherical harmonics of the operational pressure level data corresponding to a horizontal resolution of about 0.3°. With VMF1 no height correction is necessary (compare *Niell* [1996]), since the raytracing starts at the actual station height. To get the meteorological parameters at the position of each site, the temperature is interpolated linearly between the pressure levels, and the total and water vapor pressure are interpolated exponentially applying the hypsometric equation (see also [*Boehm*, 2004]). Figure 2 shows the differences of the hydrostatic delays at 5° elevation between VMF [*Boehm and Schuh*, 2004] and VMF1 (this paper) for 213 IGS (International GPS Service) stations for the day 28 in 2005 (January) and the day 210 in 2004 (July) (at 0, 6, 12, and 18 UT). It can be seen that the two hydrostatic mapping functions agree best at mid-latitudes, but that there are systematic differences closer to the equator and near the winter poles which are caused by deficiencies of the c coefficients in VMF [*Boehm and Schuh*, 2004]. These systematic errors of VMF were not detected by *Boehm and Schuh* [2004], since they made their checks only for the CONT02 stations which are situated mostly at mid-latitudes where the 'fast' VMF agrees well with the 'rigorous' approach. (For the investigations presented here, a global grid of profiles for the complete year 2001 has been used to validate VMF1.)
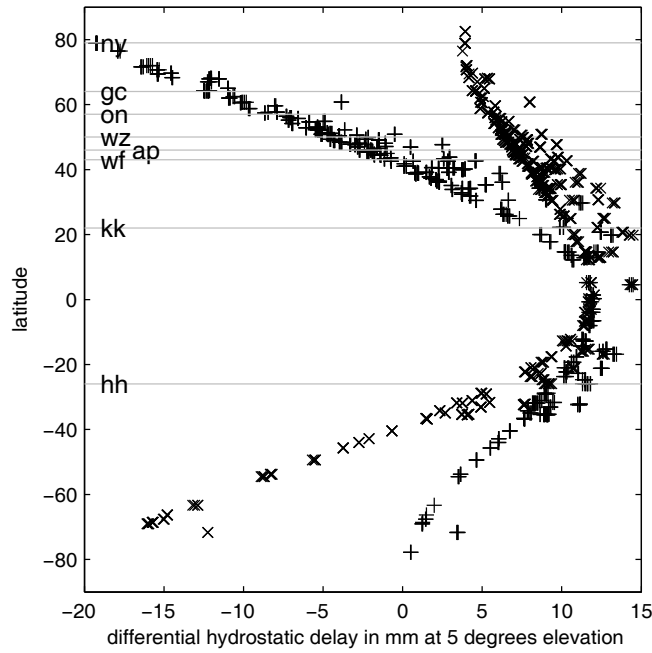
Figure 2. Hydrostatic delay differences (in mm) VMF minus VMF1 on day of year 28 in 2005 (+) and on day of year 210 in 2004 (x) at 5° elevation for 213 IGS stations. Additionally, the latitudes of the eight CONT02 stations are marked by thin horizontal lines. A differential hydrostatic delay of –20 mm at the North pole corresponds to an apparent station height change of about –4 mm when using VMF1 instead of VMF.

For the VMF [*Boehm and Schuh*, 2004], the hydrostatic b and c coefficients were taken from the Isobaric Mapping Functions IMF [*Niell and Petrov*, 2003], but it has to be mentioned that the development of IMF was based on radiosonde data which were taken mainly at mid-latitudes where the agreement between VMF and VMF1 is very good. In our work here, a global distribution was used to derive functions for the b and c coefficients, and this allowed detection of deficiencies at the winter poles and near the equator of earlier hydrostatic mapping functions.

Table 3 shows the mean biases and standard deviations of the hydrostatic delays at 5° elevation (assuming 2000 mm hydrostatic zenith delay) between reference values determined from raytracing through the numerical weather model at all grid points described at the beginning of section 2.1 and those from NMF, VMF, and VMF1, respectively. The minor standard deviation of 2 mm between the raytraced mapping function at 5° elevation and VMF1 justifies the exclusive determination of the coefficient a instead of all three coefficients a, b, and c. Contrarily, there are significant delay errors with NMF which are equivalent to station height errors of 4 mm (bias) and 7 mm (standard deviation), respectively. *Niell* [2005, personal communication], has compared VMF1 with mapping functions derived from

radiosonde data, and he found equivalent station height errors of less than 2 mm, which is similar to the values reported by *MacMillan and Ma* [1998] for differences between mapping functions from radiosonde data and numerical weather models at four selected sites.

2.3 Vienna Total Mapping Function (VMF1-T)

Instead of separating the delays into a hydrostatic and a wet part, an alternative concept of total delays has also been investigated for tropospheric modeling, that is the use of a single total mapping function mf_t (equation 5) for mapping down the a priori total zenith delays $\Delta L^z_{t,0}$ and as partial derivative for the estimation of the residual total delays $\Delta L^z_{t,res}$ (equations 8 and 9).

$$(8) \qquad \Delta L^z_t = \Delta L^z_h + \Delta L^z_w = \Delta L^z_{t,0} + \Delta L^z_{t,res}$$

$$(9) \qquad \Delta L(e) = \Delta L^z_{t,0} \cdot mf_t(e) + \Delta L^z_{t,res} \cdot mf_t(e)$$

A benefit of the numerical weather models is that they enable the determination of not only the total mapping functions (equation 5) but also of the a priori total zenith delays. Although for the analysis of VLBI sessions in section 4 a priori total zenith delays are used, a priori hydrostatic zenith delays could have been applied, too, because the mapping function for the a priori zenith delays is the same as for the residual zenith delays.

With the classical separation into a hydrostatic and a wet part, errors of the hydrostatic zenith delays cannot be fully compensated for by estimating the remaining wet part, because the hydrostatic and wet mapping functions are significantly different, especially at low elevations. The advantage of this concept is that it cannot be affected by poor a priori hydrostatic zenith delays. On the other hand, the total mapping function is close in value to the hydrostatic mapping function, which allows estimation of the residual hydrostatic delays properly only if a) the wet zenith delays have been accurately calculated from the ECMWF, and b) they do not differ from the linear interpolation between 6-hour values that is used to construct the a priori total delay.

A limitation to the concept of the total mapping function is that it is affected by bad a priori information about the wet part in the atmosphere from the numerical weather models. *Snajdrova et al.* [2005] show that the wet zenith delays determined from pressure level data of the ECMWF and the wet zenith delays estimated in the VLBI analysis for CONT02 agree at

the 1 cm level in terms of bias and up to the 2 cm level (for stations with high humidity like Kokee Park) in terms of scatter (compare table 4). While a bias of 1 cm is not that critical (corresponds to a bias of 1.2 mm in station height), a noise of about 3 mm is added to the vertical scatter at humid sites. But even if the information about the hydrostatic and wet part provided by the numerical weather models at the 6-hour time epochs was accurate at the mm level, the total mapping function would not be able to perfectly model the path delays since the variation - especially in the wet part - is more rapid than can be modeled with 6-hour time intervals (figure 3). This again adds noise to the station heights and baseline lengths (see figure 6), because the total mapping function, which is close to the hydrostatic mapping function, is not appropriate to estimate these rapid variations of the wet zenith delays.
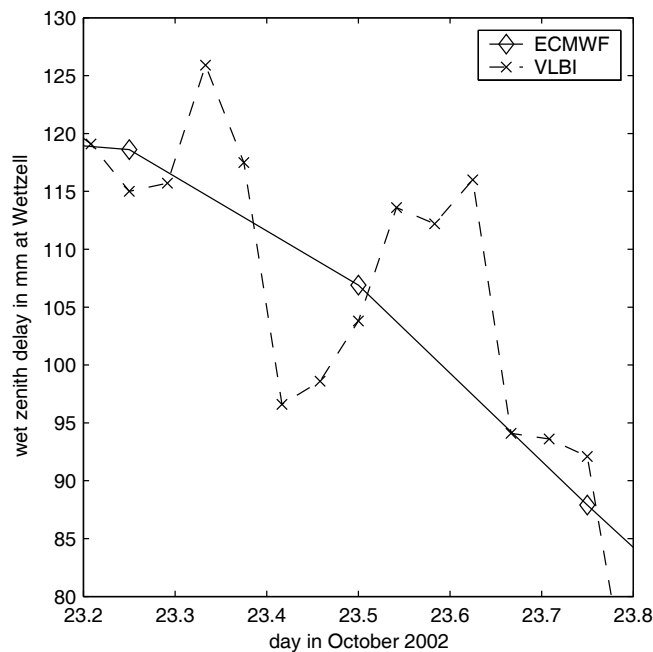

Figure 3. Wet zenith delays in mm at station Wettzell on 23 October 2002. It shows that there is more variation in the wet zenith delays than can be modeled with 6-hour data from the ECMWF.

3 A priori zenith delays

Three different methods are compared for obtaining the a priori hydrostatic zenith delays. They are determined from either of the two sources of station pressure values, or from numerical integration through pressure level data of the ECMWF. In the case of pressure values, these are taken either from the pressure sensors at the stations or from a standard model which yields the pressure for a given height h according to [*Berg*, 1948] (equation 10):
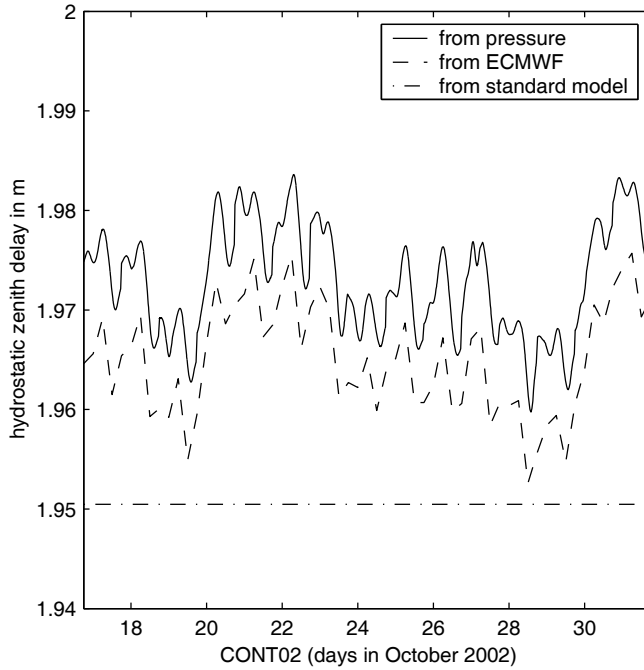
Figure 4. A priori hydrostatic zenith delays at Hartebeesthoek (South Africa) determined (1) from the pressure values at the site, (2) from ECMWF data, and (3) from a standard model for the pressure (equation 10).

$$(10) \quad p = 1013.25 \cdot (1 - 0.0000226 \cdot h)^{5.225}$$

The hydrostatic delay is then calculated using *Saastamoinen* [1973] (equation 3). Figure 4 shows the different hydrostatic zenith delays at Hartebeesthoek (South Africa) during CONT02. While the hydrostatic zenith delays derived from pressure readings at the site and those from the numerical weather model are similar (apart from a bias), the hydrostatic zenith delays from the standard model are constant with time. Table 4 summarizes the biases and standard deviations between the hydrostatic zenith delays from the observed pressure values on the one hand and those from the numerical weather model ECMWF and the standard model for the pressure on the other hand at eight VLBI sites during the CONT02 campaign.

The hydrostatic zenith delays at station Wettzell in Germany as derived from the numerical weather model are in error by about 16 mm (compared to the observed pressure values), i.e. an error of 16 mm is mapped down with the wrong mapping function. If the cutoff elevation angle is set to 5°, the delay error at 5° is 10 mm (= (10.75−10.15)·16 mm, see section 1) and the corresponding station height error is about 2 mm (compare figure 7). Thus, the error is due to using the wet mapping function with the wrong a priori zenith hydrostatic delay. At the other stations the effect is smaller. With the concept of the total mapping functions, the error

in the a priori hydrostatic zenith delays is of less importance because errors in the a priori zenith delays are corrected by estimating the residual total zenith delays (equation 9) in the least-squares fit.

However, at Wettzell for example, the wet bias of 13 mm then introduces a height error (bias) of approximately 2 mm, so the total mapping function does not significantly reduce the error even though it allows correction for the hydrostatic error. The total mapping function will in addition cause even larger errors in the total delay because of the error in the wet delay between the times of NWM input, and because the standard deviation of the wet delay from the NWM is four times larger than that of the hydrostatic delay.

Table 4. Biases and standard deviations in mm of the hydrostatic zenith delays derived from ECMWF data and the standard model for the pressure with respect to the hydrostatic zenith delays determined from the observed pressure values at eight VLBI sites in the second half of October 2002 (CONT02). The last two columns show the biases and standard deviations of the wet zenith delays between estimates from VLBI analyses and ECMWF data [Snajdrova et al., 2005].

	hydr. zenith delays [mm] (observed pressure - ECMWF)		hydr. zenith delays [mm] (observed pressure - standard model)		wet zenith delays [mm] (VLBI estimates - ECMWF)	
	bias	std.dev.	bias	std.dev.	bias	std.dev.
Algonquin Park	5	1	-8	17	-12	3
Gilmore Creek	-5	2	11	16	-8	12
Hartebeesthoek	-8	1	-23	5	-5	20
Kokee Park	-7	1	22	3	-9	21
Ny-Ålesund	-8	2	13	26	+7	5
Wettzell	-16	2	-13	16	+13	9
Westford	6	1	-5	16	-16	6
Onsala	-14	2	12	23	+8	6

4 Validation in VLBI analyses

4.1 Analysis setup

Table 5. Mapping functions which are used in the VLBI analyses of the IVS-R1 and IVS-R4 sessions of 2002 and 2003 (and CONT02). There are variations of the NMF [Niell, 1996], the VMF [Boehm and Schuh, 2004], and the VMF1 (this paper) used in combinations with different kinds of a priori zenith delays. The lowercase indices h and w refer to 'hydrostatic' and 'wet' mapping functions.

abbrev.	a priori zenith delay		mapping of	partial
	refractivity	type	a priori zenith delay	derivative
NMF	hydrostatic	pressure	NMFh	NMFw
NMF-X	hydrostatic	std. model	NMFh	NMFw
NMF-Y	total	ECMWF	NMFh	NMFh
VMF	hydrostatic	pressure	VMFh	VMFw
VMF1	hydrostatic	pressure	VMF1h	VMFw
VMF1-X	hydrostatic	ECMWF	VMF1h	VMFw
VMF1-T	total	ECMWF	VMF1-T	VMF1-T

Table 5 summarizes the mapping functions and a priori zenith delays that have been used for the analyses of all IVS-R1 and IVS-R4 sessions of 2002 and 2003 (including CONT02). NMF is the classical mapping function provided by *Niell* [1996] with the a priori hydrostatic zenith delays determined from pressure values recorded at the sites. In addition to that, two modifications of NMF are used for comparisons: NMF-X with a priori hydrostatic zenith delays determined from the standard pressure model [*Berg*, 1948], and NMF-Y with the hydrostatic NMF (NMFh) as total mapping function, i.e. NMFh is applied to map down the a priori total zenith delays from ECMWF, and as partial derivative to estimate the residual zenith delays. Both the NMF-X and NMF-Y comparisons are of interest because it is possible to select these options in some GPS software packages [*Hugentobler et al.*, 2001]. In addition to the VMF published by *Boehm and Schuh* [2004], various versions of VMF1 (this paper) are compared: VMF1 applies a priori hydrostatic zenith delays from observed pressure values at the sites, VMF1-X uses a priori hydrostatic zenith delays from ECMWF, and VMF1-T is the VMF1 for the total zenith delays as described in section 2.3.

For the geodetic VLBI analyses, the classical least-squares method (Gauss-Markov model) of the OCCAM 6.0 VLBI software package [*Titov et al.*, 2001] is used. Free network solutions with no-net translation and no-net rotation conditions [*Koch*, 1999] are calculated for the 24-hour sessions with five Earth orientation parameters being estimated (nutation, dUT1, and pole coordinates). Atmospheric loading parameters are obtained from *Petrov and Boy* [2003], and ocean loading corrections are calculated from *Scherneck and Bos* [2002] using the CSR4.0 ocean tide model by *Eanes* [1994]. The zenith delays are estimated as 1-hour continuous piecewise linear functions, and total gradients are estimated as 6-hour offsets using the model by *Davis et al.* [1993]. The cutoff elevation angle is set to 5° for all sessions.

4.2 Baseline length repeatabilities

For each baseline, the repeatability σ can be determined as the standard deviation of the n estimates b_i with regard to the mean value b_0 on a regression polynomial of first order (equation 11).

$$(11) \quad \sigma = \sqrt{\frac{\sum_{i=1}^{n}(b_i - b_0)^2}{n-2}}$$

The power of the improvement in mm^2 (reduction of variance) with a certain mapping function compared to NMF [*Niell*, 1996] is determined as the quadratic standard deviation σ^2_{NMF} minus σ^2 from the tested mapping function. For the following investigations all IVS-R1 and IVS-R4 sessions in 2002 and 2003 as well as the CONT02 sessions were analyzed, but only those 40 baselines which are made up of the eight VLBI stations which took part in CONT02 (see table 4) plus the sites Matera in Italy and Tsukub32 in Japan are shown for the statistics below.

Figure 5 shows the reduction in variance of baseline length repeatability versus baseline length. There is a clear improvement with VMF and VMF1 compared to NMF, with the largest improvements for baselines with Tsukub32 (ts). This is due to the fact that the sites in Japan do not fit into the climatological model that is inherent to NMF. Three baselines from Hartebeesthoek (South Africa) (to Kokee Park (kk), Algonquin Park (ap), and Matera (ma)) are significantly worse with both VMF and VMF1 compared to NMF. At Hartebeesthoek, it has repeatedly been seen that the results with mapping functions based on information from

the ECMWF do not surpass NMF [*Boehm and Schuh*, 2004], which might be due to rather poor ECMWF data in this region. Comparing the variances from VMF1 with those from VMF in figure 5, it is evident that VMF1 yields a slightly better precision for most of the baselines (33 out of 40).

Figure 6 shows the median reduction of variance (over all 40 baselines) in mm^2 compared to the repeatabilities from NMF. A clear improvement can be seen for VMF [*Boehm and Schuh*, 2004], and especially for all variations of VMF1. This demonstrates that there is a small improvement with the concept of the new b and c coefficients of VMF1 described in this paper, even if the stations are not situated near the equator and at the poles where the deficiencies of VMF are most critical. VMF1 is slightly degraded by introducing a priori hydrostatic zenith delays from ECMWF (VMF1-X) and even more by using the concept of the total mapping function (VMF1-T), as explained in section 2.3. NMF gives better precision over NMF-X and NMF-Y since the measured pressure (using equation 3) must give the best hydrostatic zenith delay and NMF-Y is substantially mismodeling the elevation dependence of the wet delay.
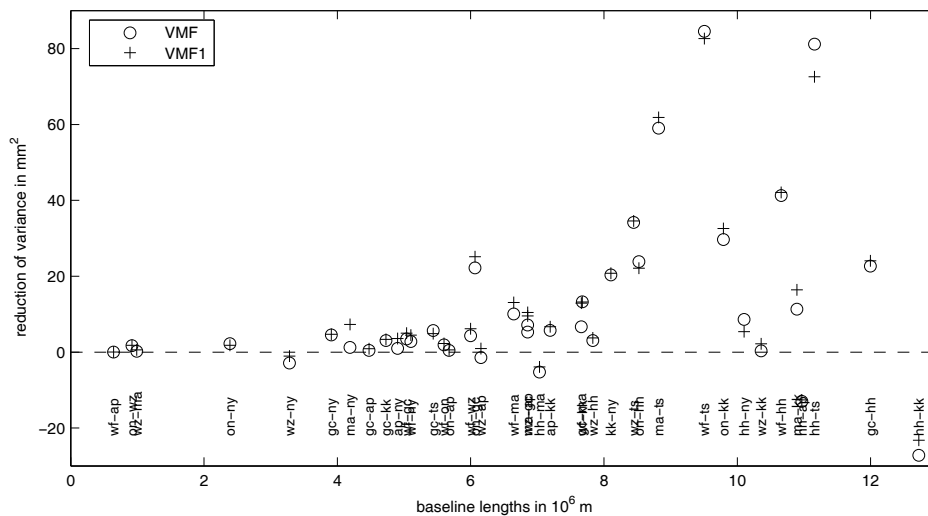

Figure 5. Variance reduction versus baseline length for all VLBI IVS-R1, IVS-R4, and CONT02 sessions in 2002 and 2003 (se text section 4.2 for baselines used). There is a clear improvement of both VMF and VMF1 compared to NMF. Only three baselines from Hartebeesthoek (to Kokee Park (kk), Algonquin Park (ap), and Matera (ma)) are significantly worse with both VMF and VMF1 compared to NMF. There is a huge improvement for baselines with the station Tsukub32 in Japan.
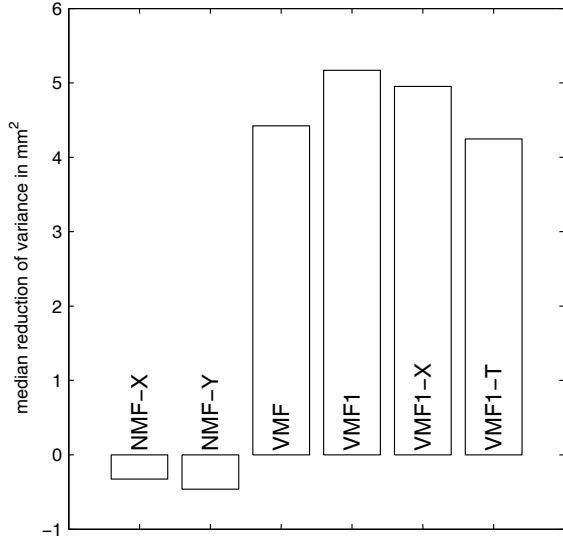
Figure 6. Median reduction of variance in mm² of the baseline length repeatabilities of all VLBI IVS-R1, IVS-R4, and CONT02 sessions in 2002 and 2003 with regard to NMF. A clear improvement is evident for VMF and all VMF1s. The best repeatability is achieved for VMF1 with the hydrostatic zenith delays determined from the observed pressure values.

4.3 Baseline lengths

The changes of the baseline lengths db can be converted into station height changes dh by using a least-squares adjustment with the Jacobian matrix based on the geometry of the baselines (equation 12).

$$(12) \quad _{40}v_1 = \begin{pmatrix} \dfrac{\partial h_1}{\partial b_1} & \dfrac{\partial h_2}{\partial b_1} & ... \\ \dfrac{\partial h_1}{\partial b_2} & \dfrac{\partial h_2}{\partial b_2} & ... \\ ... & ... & ... \end{pmatrix}_{40}^{} \cdot \begin{pmatrix} dh_1 \\ dh_2 \end{pmatrix}_{10}^{}{}_1 - \begin{pmatrix} db_1 \\ db_2 \\ ... \end{pmatrix}_{40}^{}{}_1$$

The partial derivatives in the Jacobian matrix can easily be determined with

$$(13) \quad \frac{\partial h_i}{\partial b_k} = \frac{2 \cdot R_E}{b_k},$$

when R_E is the radius of the Earth and b_k is the length of the baseline k.
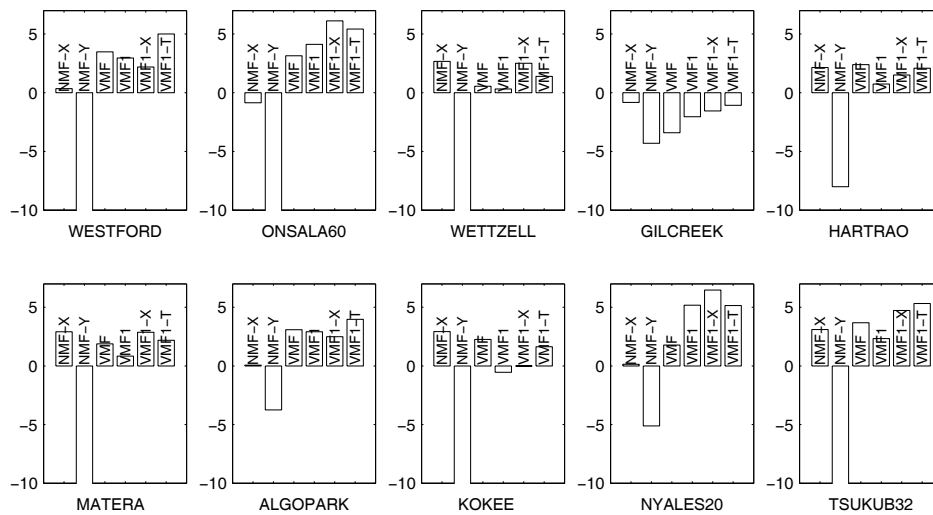
Figure 7. Changes of station heights in mm when using other mapping functions instead of NMF [Niell, 1996]. It is evident that with the hydrostatic NMF as total mapping function (denoted by NMF-Y) very poor results are obtained.
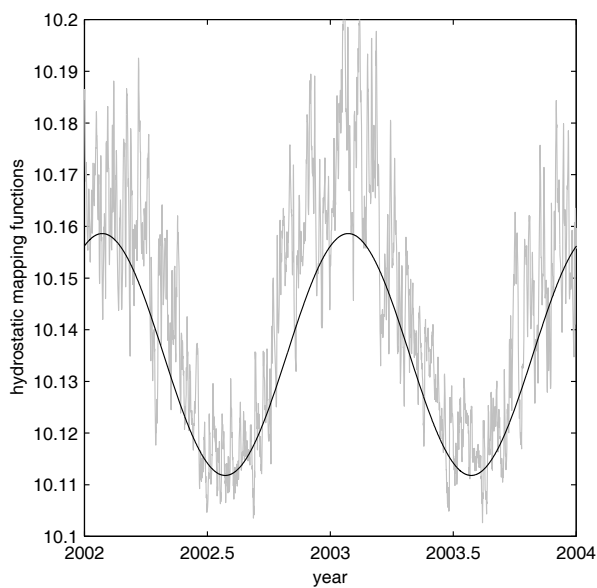

Figure 8. Hydrostatic mapping functions VMF (gray) and NMF (black) for 5° elevation at Algonquin Park (Canada) in 2002 and 2003.

Figure 7 shows the changes of the station heights determined from the changes of the mean baseline lengths (see equations 12 and 13) when using the various mapping functions instead of NMF [*Niell*, 1996]. The dominant feature in this plot is the change in baseline length when using the hydrostatic mapping function NMFh for the estimation of the total delays denoted by NMF-Y. This can be explained with the rule of thumb (see section 1), because the wet zenith delays are mapped down with the wrong mapping function. E.g., if there is a wet zenith

delay of 10 cm, the corresponding error in station height is 1.2 cm. Thus, the combination NMF-Y should never be used in GPS or VLBI analysis.

To illustrate the difference between NMF and VMF, the station Algonquin Park in Canada is used as example. As can be seen in figure 7, the station height increases by about 3 mm when using variations of VMF instead of NMF. Figure 8 shows the hydrostatic mapping function at 5° elevation for VMF and NMF in 2002 and 2003. Apart from a difference in the seasonal amplitude, a mean bias of about −0.01 can be seen between the hydrostatic mapping functions (NMFh − VMFh), which corresponds to a bias of about −2 cm between the hydrostatic delays at 5° elevation. Following the particularization of Niell's rule of thumb (see section 1), the corresponding station height change is 4 mm which is very close to the ~3 mm in figure 7.

Table 4 shows that there is a bias of −16 mm between the hydrostatic zenith delays determined from the observed pressure values at Wettzell and the hydrostatic zenith delays from ECMWF data. As indicated in section 3, this corresponds to a station height error of 2 mm for VMF1-X (compared to the VMF1 solution) if we assume the observed pressure values to be true, which is consistent with the bias shown in figure 7. To illustrate the biases between VMF and VMF1, the station Ny-Ålesund is chosen because it is situated rather close to the North pole (79° latitude) where the differences are larger than at mid-latitudes. Figure 2 shows that the differential hydrostatic delays at 5° elevation between VMF1 and VMF are −18 mm and 0 mm in January and July, respectively, corresponding to a mean difference of −9 mm over the year. Multiplied by 0.2 (the approximate ratio of the height error and the mapping function error at a 5° minimum elevation), this difference corresponds to a station height difference of ~2 mm, which is similar to the station height difference in figure 7 for Ny-Ålesund between VMF and VMF1. Similar assessments can be made for the stations Kokee Park and Hartebeesthoek.

5 Conclusions

The mapping functions NMF [*Niell*, 1996], IMF [*Niell*, 2000], and VMF [*Boehm and Schuh*, 2004] apply parameters for the b and c coefficients of the continued fraction form (equation 2) that are symmetric with regard to the equator (apart from the phase offset for the two hemispheres with NMF). In this paper it is shown that close to the equator and at high latitudes these coefficients have deficiencies, which could influence the mean station heights by as much as 4 mm. Therefore, new b and c coefficients have been developed from ERA-40 data in 2001 for the hydrostatic mapping function, and the corresponding mapping function is

referred to as VMF1. This VMF1 yields a small but significant improvement compared to the original VMF [*Boehm and Schuh*, 2004] as far as baseline length repeatabilities are concerned.

Using hydrostatic mapping functions as the partial derivatives for the estimation of total zenith delays distorts the baseline lengths considerably and thus, this approach should never be used. Alternatively, the concept of the Vienna Total Mapping Function VMF1-T is introduced which is not affected by bad a priori hydrostatic zenith delays but suffers significantly from poor a priori information about the wet part in the atmosphere. Thus, if observed pressure values are not available at the sites, VMF1-T should not be used, especially since better alternatives exist (VMF1-X).

It is shown that a priori hydrostatic zenith delays determined from raytracing through the ECMWF pressure level data can be used if no pressure values are available for a site, e.g. at GPS stations where pressure records often are not available. These a priori hydrostatic (and wet) zenith delays are provided at the webpage of the authors, http://www.hg.tuwien.ac.at/~ecmwf, for 213 IGS stations, together with the parameters of the Vienna Mapping Functions.

In the analyses of VLBI and GPS observations, there is always a trade-off between better separability of station heights, tropospheric zenith delays, and clock parameters on the one hand, and increasing mapping function errors on the other hand as observations at lower elevations are included [*MacMillan and Ma*, 1994]. New mapping functions, such as IMF, VMF, and VMF1 are required to reduce systematic errors, which is important to the geophysical use of geodesy, e.g. to detect signals in the coordinate time series that are related to hydrology. Since GPS is affected by a multitude of low-elevation error sources, such as poor or missing antenna phase center models for low elevations, the cutoff elevation angle is often set to 7° or even 10°. Then, although the differences between VMF and VMF1 might not be significant, the biases between VMF and NMF are expected to be still large enough to significantly change the station heights and, consequently, to influence the terrestrial reference frame.

Acknowledgements

manuscript. In particular, we want to thank Arthur Niell who pointed out the deficiencies of the total mapping function.

References

Berg, H., Allgemeine Meteorologie, Duemmler's Verlag, Bonn, 1948.

Boehm, J., and H. Schuh, Vienna Mapping Functions in VLBI analyses , Geophys. Res. Lett., 31, L01603, doi:10.1029/2003GL018984, 2004.

Boehm, J., Troposphärische Laufzeitverzögerungen in der VLBI, Veröffentlichung des Institutes für Geodaesie und Geophysik, Geowissenschaftliche Mitteilungen, Heft Nr. 68, ISSN 1811-8380, 2004.

Chao, C.C., The troposphere calibration model for Mariner Mars 1971, JPL Technical Report 32-1587, NASA JPL, Pasadena CA, 1974.

Davis, J.L, T.A. Herring, I.I. Shapiro, A.E.E. Rogers, and G. Elgered, Geodesy by Radio Interferometry: Effects of Atmospheric Modeling Errors on Estimates of Baseline Length, Radio Science, Vol. 20, No. 6, pp. 1593-1607, 1985.

Eanes, R.J., Diurnal and Semidiurnal tides from TOPEX/POSEIDON altimetry. Eos Trans. AGU, 75(16):108, 1994.

Hugentobler, U., S. Schaer, and P. Fridez, Bernese GPS Software Version 4.2, Astronomical Institute of the University of Berne, 2001.

Koch, K.R., Parameter Estimation and Hypothesis Testing in Linear Models, Springer, Berlin, 1999.

MacMillan, D.S., and C. Ma, Evaluation of very long baseline interferometry atmospheric modeling improvements, J. Geophys. Res., 99, B1, pp. 637-651,1994.

MacMillan, D.S., and C. Ma, Using Meteorological Data Assimilation Models in Computing Tropospheric Delays at Microwave Frequencies, Phys. Chem. Earth, Vol. 23, No. 1, pp. 97-102, 1998.

Marini, J.W., Correction of satellite tracking data for an arbitrary tropospheric profile, Radio Science, Vol. 7, No. 2, pp. 223-231, 1972.

Niell, A.E., Global mapping functions for the atmosphere delay at radio wavelengths, J. Geophys. Res., 101, B2, pp. 3227-3246,1996.

Niell, A.E., Improved atmospheric mapping functions for VLBI and GPS, Earth Planets Space, 52, pp. 699-702, 2000.

Niell, A.E., A.J. Coster, F.S. Solheim, V.B. Mendes, P.C. Toor, R.B. Langley, and C.A. Upham, Comparison of Measurements of Atmospheric Wet Delay by Radiosonde, Water Vapor Radiometer, GPS and VLBI, Journal of Atmospheric and Oceanic Technology, 18, pp. 830-850, 2001.

Niell, A.E., and L. Petrov, Using a Numerical Weather Model to Improve Geodesy, in Proceedings: The State of GPS Vertical Positioning Precision: Separation of Earth Processes by Space Geodesy, April 2-4, 2003, Luxembourg, 2003.

Petrov, L., and J.P. Boy, Study of atmospheric pressure loading signal in VLBI observations, Journal of Geophysical Research, 10.1029/2003JB002500, 2003.

Saastamoinen, J., Contributions to the Theory of Atmospheric Refraction, Part II, Bulletin Geodesique, Vol. 107, pp. 13-34, 1973.

Snajdrova, K., J. Boehm, P. Willis, R. Haas, and H. Schuh, Multi-technique comparison of tropospheric zenith delays derived during the CONT02 campaign, accepted by Journal of Geodesy, 2005.

Scherneck, H.-G., and M.S. Bos, Ocean Tide and Atmospheric Loading, International VLBI Service for Geodesy and Astrometry 2002 General Meeting Proceedings, edited by Nancy R. Vandenberg and Karen D. Baver, NASA/CP-2002-210002, 205-214, 2002.

Simmons, A.J., and J.K. Gibson (editors), The ERA-40 Project Plan, ERA-40 Project Report Series No. 1, http://www.ecmwf.int, 2000.

Thomas, C., and D.S. MacMillan, Core Operation Center Report, in International VLBI Service for Geodesy and Astrometry 2002 Annual Report, edited by N. R. Vandenberg and K. D. Baver, NASA/TP-2003-211619, 2003.

Titov, O., V. Tesmer, and J. Boehm, Occam Version 5.0 Software User Guide, AUSLIG Technical Report 7, 2001.